Title

Elucidation of Primary Structure Elements Controlling Early Amyloid β-Protein Oligomerization*

Journal

Journal of Biological Chemistry, 278(37)

ISSN

0021-9258

Authors

Bitan, Gal
Vollers, Sabrina S
Teplow, David B

Publication Date

2003-09-01

DOI

10.1074/jbc.m300825200

Peer reviewed

THE JOURNAL OF BIOLOGICAL CHEMISTRY
Vol. 278, No. 37, Issue of September 12, pp. 34882–34889, 2003
Printed in U.S.A.

Elucidation of Primary Structure Elements Controlling Early Amyloid β-Protein Oligomerization*[S]

Received for publication, January 24, 2003, and in revised form, June 10, 2003
Published, JBC Papers in Press, July 1, 2003, DOI 10.1074/jbc.M300825200

Gal Bitan, Sabrina S. Vollers, and David B. Teplow‡

From the Center for Neurologic Diseases, Brigham and Women's Hospital, and Department of Neurology, Harvard Medical School, Boston, Massachusetts 02115

Assembly of monomeric amyloid β-protein (Aβ) into oligomeric structures is an important pathogenetic feature of Alzheimer's disease. The oligomer size distributions of aggregate-free, low molecular weight Aβ40 and Aβ42 can be assessed quantitatively using the technique of photo-induced cross-linking of unmodified proteins. This approach revealed that low molecular weight Aβ40 is a mixture of monomer, dimer, trimer, and tetramer, in rapid equilibrium, whereas low molecular weight Aβ42 preferentially exists as pentamer/hexamer units (paranuclei), which self-associate to form larger oligomers. Here, photo-induced cross-linking of unmodified proteins was used to evaluate systematically the oligomerization of 34 physiologically relevant Aβ alloforms, including those containing familial Alzheimer's disease-linked amino acid substitutions, naturally occurring N-terminal truncations, and modifications altering the charge, the hydrophobicity, or the conformation of the peptide. The most important structural feature controlling early oligomerization was the length of the C terminus. Specifically, the side-chain of residue 41 in Aβ42 was important both for effective formation of paranuclei and for self-association of paranuclei into larger oligomers. The side-chain of residue 42, and the C-terminal carboxyl group, affected paranucleus self-association. Aβ40 oligomerization was particularly sensitive to substitutions of Glu^{22} or Asp^{23} and to truncation of the N terminus, but not to substitutions of Phe^{19} or Ala^{21}. Aβ42 oligomerization, in contrast, was largely unaffected by substitutions at positions 22 or 23 or by N-terminal truncations, but was affected significantly by substitutions of Phe^{19} or Ala^{21}. These results reveal how specific regions and residues control Aβ oligomerization and show that these controlling elements differ between Aβ40 and Aβ42.

Past studies of the role of the amyloid β-protein (Aβ)[1] in Alzheimer's disease (AD) have linked the neurotoxicity of Aβ with its tendency to form amyloid fibrils (1–4). However, accumulating evidence suggests that soluble Aβ oligomers and prefibrillar aggregates are the proximal effectors of neurotoxicity in early stages of AD (for reviews, see Refs. 5–7). Soluble oligomeric forms of Aβ, including dimers and trimers (8, 9), Aβ-derived diffusible ligands (10–16), and protofibrils (17–20) are neurotoxic. Transgenic mice expressing the human amyloid β-protein precursor (AβPP) exhibit neurologic deficits prior to the appearance of amyloid deposits (21–23). In humans, Aβ oligomers have been detected in cerebrospinal fluid of Alzheimer's patients but not in age-matched controls (24). An AβPP mutation causing reduction of total Aβ levels accompanied by accelerated Aβ assembly into protofibrils has been linked to early onset familial Alzheimer's disease (FAD) in a Swedish kindred (25). These findings support an important role for Aβ oligomers in the etiology of AD and thus make Aβ oligomers attractive therapeutic targets.

If effective drug design strategies targeting Aβ oligomers are to be developed, detailed knowledge of the structures and assembly dynamics of these oligomers must be obtained. However, the biophysical and structural characterization of oligomeric Aβ assemblies has been difficult due to their metastable nature. Previously, we demonstrated that the size distribution of Aβ oligomers could be determined quantitatively (26, 27) using the technique photo-induced cross-linking of unmodified proteins (PICUP) (28, 29). This approach revealed that low molecular weight (LMW) Aβ40, rather than existing in a stable monomeric or dimeric state, as previously suggested (30, 31), comprised a mixture of monomer, dimer, trimer, and tetramer in rapid equilibrium. In contrast, LMW Aβ42 produced a distinct oligomer distribution in which the main components were pentamer/hexamer units (paranuclei), which then formed larger oligomers through self-association (27). Here, PICUP was used to determine systematically the effects of primary structure modifications on early Aβ oligomerization. We studied Aβ42 analogues bearing modifications at the C-terminal dipeptide, Aβ40 and Aβ42 analogues containing clinically relevant mutations at or near the central hydrophobic cluster (CHC), N-terminally truncated alloforms of Aβ40 and Aβ42 found in amyloid plaques, and Aβ40 analogues containing substitutions that alter the net charge of the peptide. The results advance our understanding of early Aβ assembly, provide deeper mechanistic insight into the distinct oligomerization behaviors of Aβ40 and Aβ42, and suggest new targets for AD therapy.

* This work was supported by grants AG18921 and NS38328 from the National Institute of Health (to D. B. T.), by the Foundation for Neurologic Diseases (to D. B. T.), and by Grant 1042312909A1 from The Massachusetts Alzheimer's Disease Research Center (to G. B.). The costs of publication of this article were defrayed in part by the payment of page charges. This article must therefore be hereby marked "*advertisement*" in accordance with 18 U.S.C. Section 1734 solely to indicate this fact.

[S] The on-line version of this article (available at http://www.jbc.org) contains figures of densitometric analysis.

‡ To whom correspondence should be addressed: Center for Neurologic Diseases, Brigham and Women's Hospital, 77 Ave. Louis Pasteur (HIM 756), Boston, MA 02115-5716. Tel.: 617-525-5270; Fax: 617-525-5252; E-mail: teplow@cnd.bwh.harvard.edu.

[1] The abbreviations used are: Aβ, amyloid β-protein; AβPP, amyloid β-protein precursor; AD, Alzheimer's disease; CHC, central hydrophobic cluster; FAD, familial Alzheimer's disease; LMW, low molecular weight; NTT, N-terminally truncated; PICUP, photo-induced cross-linking of unmodified proteins; Ru(Bpy), Tris(2,2′-bipyridyl)dichlororuthenium(II); SEC, size exclusion chromatography; WT, wild type.

MATERIALS AND METHODS

Peptides and Reagents—Aβ40, Aβ42, and analogues thereof (Table I) were synthesized by Fmoc (*N*-(9-fluorenyl)methoxycarbonyl) chemistry, purified by reversed-phase high performance liquid chromatography, and characterized by mass spectroscopy and amino acid analysis, as described (32). Tris(2,2′-bipyridyl)dichlororuthenium(II) (Ru(Bpy)) and ammonium persulfate were purchased from Aldrich. Polyacrylamide gels, buffers, stains, standards, and equipment for SDS-PAGE were from Invitrogen.

Isolation of LMW Aβ—LMW fractions of Aβ alloforms were isolated by size exclusion chromatography (SEC), as described previously (26). Briefly, 170 μl of a 2 mg/ml peptide solution prepared in Me_2SO was fractionated using a 10/30 Superdex 75 HR column eluted at 0.5 ml/min with 10 mM sodium phosphate, pH 7.4. Peaks were detected by UV absorbance at 254 nm. A 10-μl aliquot of each fraction was taken for amino acid analysis *a posteriori* to determine the peptide concentration. Typical concentrations were 30 ± 10 μM. SEC reproducibly yielded comparable LMW fractions for all of the peptides used. Recent studies (27) have shown that LMW Aβ prepared using SEC readily forms paranuclei and higher order oligomers, facilitating study of these assembly processes. For this purpose, SEC was superior to base pretreatment protocols (34).

Cross-linking and SDS-PAGE Analysis—Freshly isolated LMW peptides were immediately subjected to PICUP, as described (26). Briefly, 1 μl of 1 mM Ru(Bpy) and 1 μl of 20 mM ammonium persulfate in 10 mM sodium phosphate, pH 7.4, were added to 18 μl of freshly isolated LMW peptide. The mixture was irradiated for 1 s with visible light, and the reaction was quenched immediately with 10 μl tricine sample buffer (Invitrogen) containing 5% β-mercaptoethanol. Concentration differences caused some variability in the relative abundance of each oligomer but did not alter the overall profile of the oligomer size distribution of each peptide (26). To examine further the question of whether inter-peptide oligomerization differences reflected fundamental differences in peptide assembly and not simply the effects of differing peptide concentrations, a series of cross-linking experiments were performed using Aβ40 and Aβ42 at varying concentrations. At all concentrations, from 1–300 μM, the oligomer size distributions of Aβ40 were distinct from those of Aβ42 (data not shown). This confirmed that the assembly differences we observed in the experiments reported here, and in prior work (26, 27), reflected fundamental differences between peptides and not concentration effects.

In principle, radical formation may occur at any site along the polypeptide chain. However, the radical would form at, and further react preferentially with, amino acid side-chains that offer stabilization through aromatic or neighboring-group effects (*e.g.* Tyr, Phe, or Met (35). The primary factors determining how Aβ is cross-linked are the proximity of a susceptible group to the radical and the lifetime of the radical itself. If the lifetime of the radical is long enough to allow intermolecular cross-linking as opposed to quenching by solvent, then the actual chemical nature of the radical is relatively unimportant. Cross-linked Aβ samples were analyzed by SDS-PAGE and silver staining, as described previously (26). The nominal total amount of peptide in each lane of the gels was identical. Gels were dried, scanned, and the intensities of the resulting monomer and oligomer bands quantified by densitometry using the program One-Dscan (Scanalytics, Fairfax, VA). The densitometric data for each of the figures is available as supporting online material. The relative amount of each band, as a percentage of all bands, was determined by calculating the quotient of its intensity and the sum of all band intensities and then multiplying by 100.

RESULTS

Effects of Structural Modifications at the C Terminus of Aβ42 on Oligomerization—Our previous studies (26, 27) revealed that LMW Aβ40 and Aβ42 had distinct oligomer size distributions. LMW Aβ40 existed as an equilibrium mixture of monomer, dimer, trimer, and tetramer (26). In contrast, LMW Aβ42 comprised three groups of oligomers: 1) monomer through trimer, displaying decreasing intensity with increasing oligomer order; 2) a Gaussian-like distribution between tetramer and octamer, with a maximum at pentamer and hexamer; and 3) oligomers of M_r ~30–60 kDa, among which two intensity maxima, at dodecamer and octadecamer, were observed (27). These higher order oligomers appeared to form through self-association of pentamer/hexamer units (paranuclei). The data demonstrated that Ile^{41} was essential for formation of paranuclei, whereas Ala^{42} was required for rapid self-association of paranuclei into larger oligomers (27). To better understand how amino acid side-chain structure in the C-terminal dipeptide of Aβ42 controls oligomerization, seven peptide alloforms (C terminus, Table I) were prepared and their oligomer size distributions were determined by PICUP/SDS-PAGE (Fig. 1).

Substitution of Ile^{41} by Gly, eliminating both the side-chain and the stereocenter of the Cα group, yielded a distribution that was qualitatively similar to that of Aβ40 (26) (*cf.* Fig. 1, *lane 2* and Fig. 2*A*, *lane 1*). Monomer through trimer formed in similar amounts, and a rapid decrease in oligomer abundance was observed above trimer, whereas Aβ40 showed abundant tetramer, above which abundances decreased. [Gly^{41}]Aβ42 thus existed in a dynamic equilibrium involving monomer, dimer, and trimer, but not tetramer (the mathematical foundation for this analysis has been published (26)). When Ile^{41} was substituted by Ala, dimer and trimer were the predominant cross-linking products, a characteristic of Aβ40 distributions. However, in contrast to wild type (WT) Aβ40 distributions, tetramer abundance was low, whereas pentamer abundance was relatively high. This polytonic distribution is characteristic of Aβ42. The oligomer size distribution of [Ala^{41}]Aβ42 thus appeared to be a composite of Aβ40- and Aβ42-like distributions. The majority of the peptide existed as an equilibrium mixture of monomer, dimer, and trimer, as in the case of [Gly^{41}]Aβ42, but the methyl side-chain of Ala^{41} facilitated limited paranucleus formation. Substitution of Ile^{41} by Val or Leu led to formation of abundant paranuclei. However, in the oligomer size distribution of [Val^{41}]Aβ42, no oligomers at ~30–60 kDa were detected. In the distribution of [Leu^{41}]Aβ42 the amount of these high molecular weight oligomers was substantially reduced relative to that of WT Aβ42. Consistent with the low amounts of high molecular weight oligomers, a higher abundance of dimer and trimer were observed for [Val^{41}]Aβ42 and [Leu^{41}]Aβ42 (~18% dimer and ~14% trimer for each) relative to WT Aβ42 (~14% dimer and ~10% trimer), demonstrating that these oligomers were in equilibrium with tetramer through octamer. Thus, the side-chain in position 41 is involved in the formation and self-association of Aβ42 paranuclei. Examination of the distributions produced by Gly^{41}-, Ala^{41}-, and Val^{41}-substituted Aβ42 reveals a correlation between paranucleus formation and side-chain size. [Val^{41}]Aβ42 and [Leu^{41}]Aβ42, containing iso-propyl and iso-butyl side-chains, respectively, do not facilitate self-association of paranuclei, whereas the *sec*-butyl side-chain of Ile does.

Substitution of Ala^{42} by Gly or Val had little effect on formation of paranuclei (Fig. 1). However, no high molecular mass oligomers (~30–60 kDa) were observed for [Gly^{42}]Aβ42, demonstrating a role for the methyl side-chain of Ala^{42} in the self-association of paranuclei. When the C-terminal carboxyl group was replaced by a carboxamide, a large increase in the abundance of high molecular weight oligomers was seen (Fig. 1). Thus, hydrophobic interactions involving the side-chains in residues 41 and 42 appear to be a driving force in the association of Aβ42 paranuclei into higher oligomers, whereas the C-terminal carboxylate anion moderates this assembly effect.

Effects of Structural Modifications in the Central Region of Aβ on Oligomerization—Five naturally occurring, autosomal dominant mutations in the AβPP gene region encoding the CHC of amino acids in Aβ have been reported (25, 36–40). All result in cerebrovascular or parenchymal amyloid deposition, leading to AD-like diseases often characterized by recurrent cerebral hemorrhage. The mutations are thought to cause disease through alteration of AβPP processing or Aβ aggregation kinetics (due to the resulting amino acid substitutions) (41, 42).

TABLE I
Aβ peptides: primary structure and isoelectric point (pI)[a]

Group	Position	Modification[b]	Aβ40[c]	Aβ42[c]	pI[d]
N terminus	1-2	Δ	+	+	5.77
	1-2	Δ, <Glu^{3}	+	−	6.03
	1-4	Δ	+	+	6.30
	1-9	Δ	+	+	6.03
	1-10	Δ	+	+	6.03
	1-10	Δ, <Glu^{11}	+	−	6.03
Central region	Phe^{19}	Pro	+	+	5.22
	Ala^{21}	Gly (Flemish)	+	+	5.22
	Glu^{22}	Gly (Arctic)	+	+	5.76
	Glu^{22}	Gln (Dutch)	+	+	5.76
	Glu^{22}	Lys (Italian)	+	+	6.31
	Asp^{23}	Asn (Iowa)	+	+	5.77
C terminus	Ile^{41}	Gly	−	+	5.22
	Ile^{41}	Ala	−	+	5.22
	Ile^{41}	Val	−	+	5.22
	Ile^{41}	Leu	−	+	5.22
	Ala^{42}	Gly	−	+	5.22
	Ala^{42}	Val	−	+	5.22
	−COOH	−CONH2	−	+	5.77
Asp/His	Asp^{1}	Asn	+	−	5.77
	Asp^{7}	Asn	+	−	5.77
	Asp^{23}	Asn	+	−	5.77
	His^{6}	Gln	+	−	4.74
	His^{13}	Gln	+	−	4.74
	His^{14}	Gln	+	−	4.74
	Asp$^{1, 7, 23}$	Asn	+	−	7.26
	His$^{6, 13, 14}$	Gln	+	−	4.08
	Asp$^{1, 7, 23}$ His$^{6, 13, 14}$	Asn$^{1, 7, 23}$ Gln$^{6, 13, 14}$	+	−	6.36

[a] The WT Aβ42 sequence is: *(H)-DAEFRHDSGYEVHHQKLVFFAEDVSGNKGAIIGLMVGGVVIA-(OH)*.
[b] The symbols Δ and < signify amino acid deletion and pyroglutamyl N terminus, respectively. The common name for each mutation is listed parenthetically.
[c] The columns indicate on which backbone the primary structure changes were made. The symbols + and − signify whether the specific peptide was or was not studied.
[d] Isoelectric point (pI) values were estimated using MacVector, v. 7.1 (Accelrys, San Diego, CA).

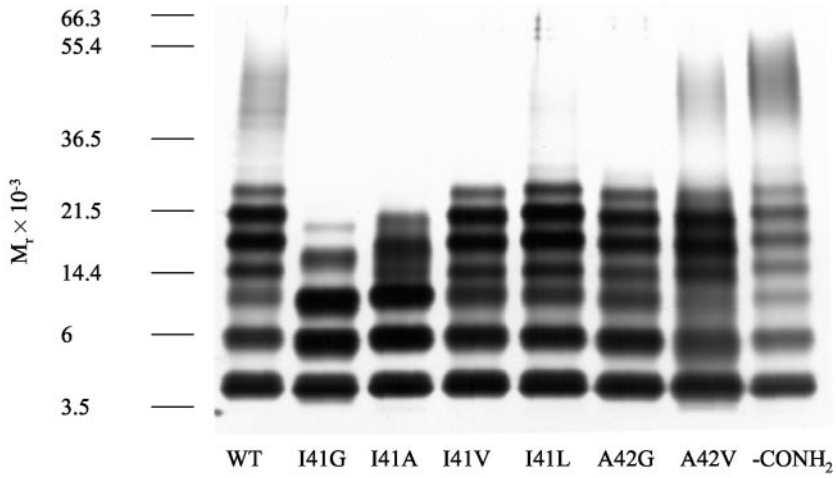

FIG. 1. **Effects of C terminus structure on paranucleus formation and assembly.** PICUP was applied to LMW Aβ42 analogues containing the modifications Ile^{41} → Gly, Ile^{41} → Ala, Ile^{41} → Val, Ile^{41} → Leu, Ala^{42} → Gly, Ala^{42} → Val, or Aβ42-carboxamide. WT Aβ42 was used as control. Molecular weight markers are shown on the *left*. The gel is representative of each of 3 independent experiments. The densitometric analysis of these experiments is available as supporting online material.

The substitutions include Ala^{21} → Gly, associated with a familial form of cerebral amyloid angiopathy in a Flemish kindred (36); Glu^{22} → Gln, which causes hereditary cerebral hemorrhage with Amyloidosis-Dutch type (37); Glu^{22} → Lys, which is associated with cerebral amyloid angiopathy and hemorrhagic stroke in an Italian kindred (38); Glu^{22} → Gly, the "Arctic" mutation, which was linked to early onset AD in a Swedish kindred (25, 39); and Asp^{23} → Asn, recently discovered in an Iowa family and found to cause severe, early onset cerebral amyloid angiopathy (33, 40). Aβ congeners bearing these mutations display distinct aggregation kinetics. The rate of fibril formation by the Flemish and Italian mutants is decreased relative to WT Aβ (43, 44), whereas the Dutch and Iowa mutant peptides form fibrils substantially faster (33, 44). The Arctic peptide does not show an overall change in the rate of fibrillogenesis relative to WT Aβ40, but rather accelerated protofibril formation (25). In addition to these five naturally occurring Aβ alloforms, a Phe^{19} → Pro substitution has been shown to prevent fibril formation *in vitro* (45, 46). Each of these Aβ alloforms was synthesized on both Aβ40 and Aβ42 backbones to determine how Aβ central region structure controls oligomerization (Table I, Central Region).

LMW Aβ preparations from each peptide were isolated, cross-linked, and analyzed by SDS-PAGE. Aβ40 alloforms displayed distributions characterized by intense monomer through tetramer bands, followed by a sharp exponential decrease in the levels of higher order oligomers (Fig. 2*A*). The two substitutions lying within the CHC, Phe^{19} → Pro and Ala^{21} → Gly, had little effect on the oligomer distribution. This result was particularly unexpected for the non-fibrillogenic Phe^{19} → Pro alloform. We have shown that monomeric peptides, when subjected to PICUP, yield oligomer distributions

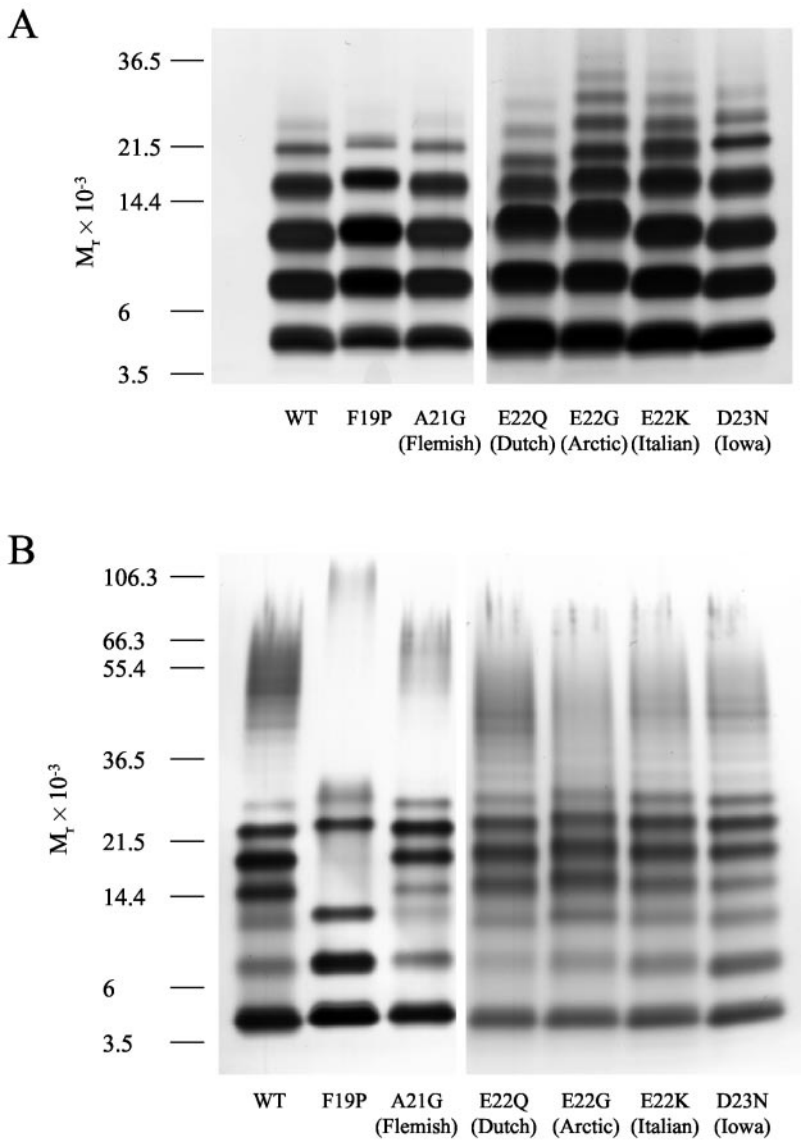

FIG. 2. **Effects of central region structure on early Aβ assembly.** LMW Aβ40 (*A*) and Aβ42 (*B*), each containing the substitutions $Phe^{19} \rightarrow Pro$, $Ala^{21} \rightarrow Gly$, $Glu^{22} \rightarrow Gln$, $Glu^{22} \rightarrow Gly$, $Glu^{22} \rightarrow Lys$, or $Asp^{23} \rightarrow Asn$, were cross-linked, analyzed by SDS-PAGE, and visualized by silver staining. WT Aβ40 and Aβ42 were used as controls. Molecular weight markers are shown on the *left* of each *panel*. The gels are representative of each of 6 independent experiments. The densitometric analysis of these experiments is available as supporting online material.

characterized by a shallow exponential decrease in oligomer abundance starting at monomer or dimer and extending up to dodecamer or tridecamer (26). The distribution obtained for the $[Pro^{19}]$Aβ40 indicates that although this analogue does not form fibrils, it associates into small oligomers in a manner similar to WT Aβ40. Despite the similarity in the oligomer size distribution between the WT and the Pro^{19}-substituted analogue, the gel mobilities of $[Pro^{19}]$Aβ40 oligomers were lower than those of WT Aβ40 oligomers. This result is consistent with disruption of a putative compact structure of the CHC of WT Aβ40 by the $Phe^{19} \rightarrow Pro$ substitution. All the peptides with substitutions at positions 22 or 23, particularly $[Gly^{22}]$Aβ40, produced distributions extending to relatively high oligomer order. The distributions reflect the increased propensity of these analogues to form higher order oligomers and suggest an important role for Glu^{22} and Asp^{23} in controlling Aβ40 oligomerization. The gel mobilities of tetrameric and higher order oligomers of Aβ analogues containing substitutions at Glu^{22} were larger than those of the counterpart WT Aβ40 oligomers, suggesting that the substitutions facilitated formation of a compact structure in the resulting oligomers.

The Aβ42 (Fig. 2*B*) alloforms generally displayed polytonic distributions characterized by decreasing band intensities from monomer to trimer, a Gaussian-like distribution of intensities centered at pentamer/hexamer, and finally, a group of higher molecular weight oligomers. The distribution obtained for $Ala^{21} \rightarrow Gly$ was qualitatively similar to that of the WT. However, the distribution of paranuclei was narrower than that of WT Aβ42, and densitometric analysis revealed that the relative abundance of paranuclei in the $[Gly^{21}]$Aβ42 distribution was 25%, compared with a relative abundance of 16% for WT paranuclei. Higher molecular mass oligomers of the Flemish mutant were centered at ~60 kDa, compared with those of WT Aβ40, which were centered at ~50 kDa. The relative abundances of the high molecular weight oligomers were 25 and 48% for the Flemish and WT Aβ42 peptides, respectively. The Flemish mutation thus appears to facilitate paranucleus formation. The higher oligomers formed by self-assembly of the Flemish paranuclei are larger, on average, than those formed by WT Aβ42, but their rate of formation is lower. The data are consistent with the lower rate of fibril formation reported for the $Ala^{21} \rightarrow Gly$ mutant relative to WT Aβ (30, 46, 47). The distribution of $[Pro^{19}]$Aβ42 comprised primarily monomer, dimer, trimer, hexamer, and a small amount of heptamer. Little or no tetramer and pentamer were observed. Higher order assemblies also formed, but unlike those of WT Aβ42 and the other alloforms, which ranged in molecular mass from ~40–80 kDa, those of the $[Pro^{19}]$Aβ42 peptide had molecular masses of ~120–150 kDa (Fig. 2*B*). Substitutions at positions 22 or 23 produced distributions of monomer through octamer, which

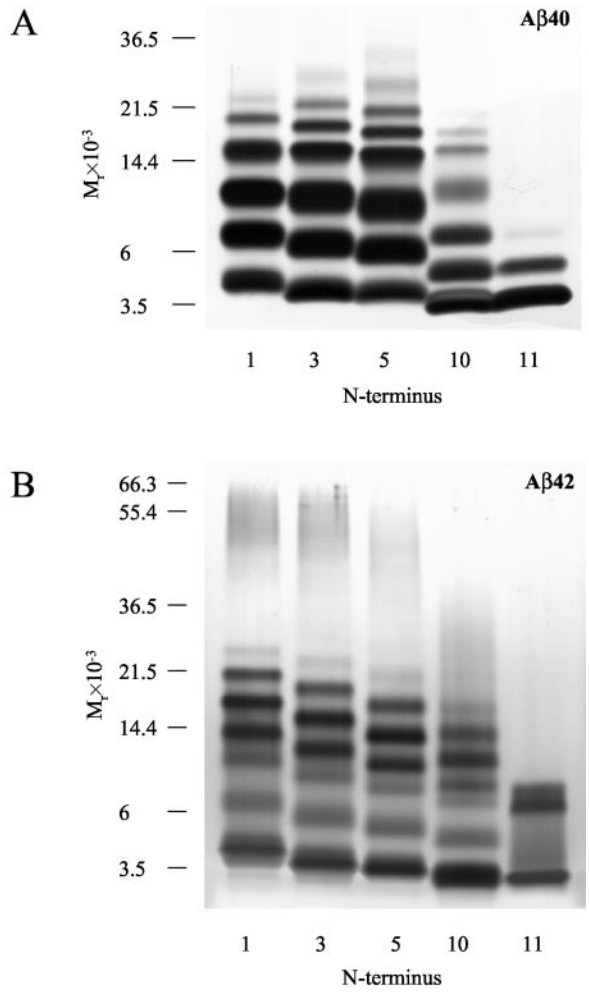

FIG. 3. **Effects of N terminus structure on early Aβ assembly.** LMW Aβ(*X*-40) (*A*) and Aβ(*X*-42) (*B*), in which *X* = 1, 3, 5, 10, or 11, were cross-linked, analyzed by SDS-PAGE, and the resulting bands visualized by silver staining. Molecular weight markers are shown on the *left* of each *panel*. The gels are representative of each of 4 independent experiments. The densitometric analysis of these experiments is available as supporting online material.

were similar to that produced by WT Aβ42. However, the intense bands of high order oligomers observed at $M_r \approx 45$–70 kDa with the WT peptide were substantially less intense in the Glu^{22}- and Asp^{23}-substituted alloforms.

Effect of N-terminal Truncations on Aβ Oligomerization—N-terminally truncated (NTT) Aβ is found in significant amounts in amyloid plaques (48, 49). In addition, cell culture studies have shown that NTT-Aβ peptides are secreted as a part of normal cellular metabolism (50, 51). Thus, NTT-Aβ has been hypothesized to have a role in the etiology of AD (49, 50, 52–54). The most abundant NTT-Aβ analogues found in AD plaques are those beginning at Glu^3, Arg^5, or Glu^{11} (41, 53). Therefore, the oligomer size distributions of analogues starting at these positions and ending either at Val^{40} or Ala^{42} were analyzed (N terminus, Table I). In Aβ(11–40) and Aβ(11–42), Tyr, one of the most reactive residues in radical cross-linking reactions (35), is missing. Therefore, to evaluate the relative contribution of Tyr^{10} to the observed profile of PICUP-generated Aβ oligomers, Aβ (10–40) and Aβ(10–42) also were included.

Deletion of Asp^1 and Ala^2 of Aβ40 (Fig. 3*A*) led to extension of the observed oligomer distribution up to an octamer. Deletion of two additional residues, Glu^3 and Phe^4, extended the size distribution to nonamer. An irregular distribution was obtained for Aβ(10–40). The distribution extended to heptamer and contained a two-color monomer band and a broad, nebulous tetramer band. The cross-linking yield ($(A\beta_{total} - A\beta_{monomer})/(A\beta_{total})$) was lower in the absence of Tyr^{10}. Approximately 40% of Aβ(11–40) were cross-linked, compared with ~70% for Aβ(10–40), and the highest order oligomer observed was a trimer. In contrast to the effects of N-terminal deletions on the distribution of Aβ(*X*–40) peptides, the same deletions had little effect on the oligomer size distributions of Aβ(*X*–42) analogues, with the exception of Aβ(11–42) (Fig. 3*B*). The Aβ(*X*-42) peptides beginning at Glu^3, Arg^5, or Tyr^{10} showed oligomer distributions essentially identical to that of Aβ42, albeit of lower M_r. Somewhat reduced amounts of high molecular weight oligomers were observed for Aβ(3–42) and Aβ(5–42). These results demonstrate the primacy of the C terminus of Aβ42 in oligomerization. As observed for Aβ40, deletion of Tyr^{10} decreased the cross-linking yield, and in addition produced a pronounced, nebulous, trimer band, which has been shown previously to be an SDS-induced artifact (27).

A significant portion of NTT-Aβ peptides found within amyloid deposits *in vivo* begins with pyroglutamylated (<Glu) Glu^3 or Glu^{11} (55, 56). Therefore, the effects of these post-translational modifications were examined. An Aβ40 backbone was used because it was found to be sensitive to N-terminal structure modifications (Fig. 3*A*). The oligomer size distributions of cross-linked oligomers produced by [<Glu^3]Aβ(3–40) or [<Glu^{11}]Aβ(11–40) were identical to those of their uncyclized homologues (data not shown).

Effects of Charge-altering Substitutions on Aβ Oligomerization—The results obtained for Aβ analogues containing substitutions of Glu^{22} or Asp^{23} (Fig. 2*A*), or N-terminal deletions (Fig. 3*A*), revealed that Coulombic interactions may be particularly important in Aβ40 oligomerization. Recently, based on solid state NMR data (57), a salt bridge between Asp^{23} and Lys^{28} has been implicated in stabilizing a turn structure in Aβ40 fibrils. This salt bridge, and other ionic interactions, may occur during the initial oligomerization of Aβ, before extensive β-sheet structures form. Thus, amino acid substitutions altering charged residues may provide information about specific Coulombic interactions involved in early Aβ assembly. Charge alterations also change the isoelectric point (pI) of the protein. Substitutions raising the Aβ pI, estimated to be 5.2–5.5 (58–60), could facilitate peptide aggregation at physiologic pH. In addition, substitutions of Asp or His residues previously have been shown to retard the formation of an α-helix-rich, oligomeric assembly intermediate, possibly by stabilizing structures that precede the α-helix-rich intermediate (61).

To examine systematically the effects of charge neutralization on Aβ oligomerization, Asp → Asn and His → Gln substitutions were incorporated into Aβ40. The substitutions included $Asp^1 \rightarrow Asn$, $Asp^7 \rightarrow Asn$, $Asp^{23} \rightarrow Asn$, $His^6 \rightarrow Gln$, $His^{13} \rightarrow Gln$, or $His^{14} \rightarrow Gln$ (Asp/His, Table I). The strategy for selecting the substitutions was based upon theoretical considerations of protein evolution and chemical biology, as well as results of published experimental work (61). Each peptide was cross-linked, and the products were analyzed by SDS-PAGE. In addition, analogues containing substitution of all three Asp residues, all three His residues, or all Asp and all His residues, were also examined. Substitution of all three Asp residues promoted formation of oligomers extending at least to undecamer (Fig. 4). Analogues containing single Asp → Asn substitutions displayed oligomer size distributions similar to that of WT Aβ40. The formation of higher order oligomers by the triply substituted analogue may be related to the change in its pI, to ~7.3, a value almost identical to the pH of the medium, 7.4. A similar distribution was obtained for the analogue in

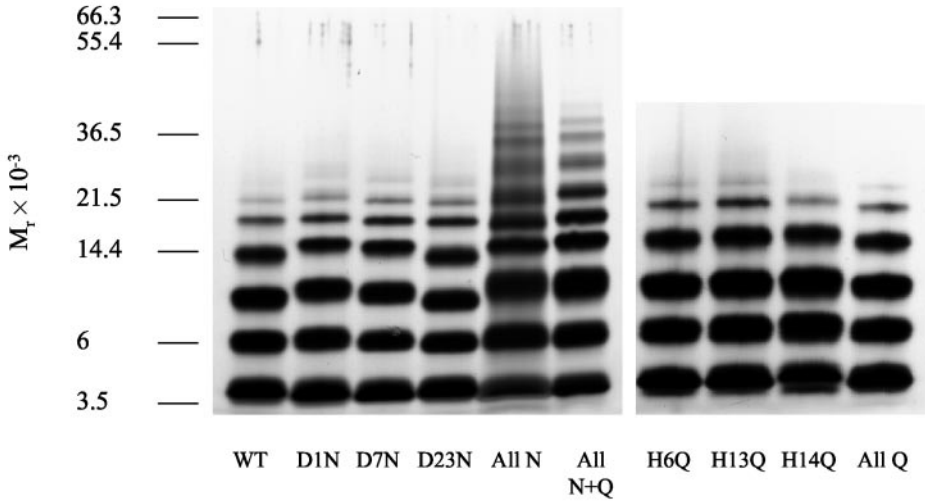

FIG. 4. **Effects of charged residue substitutions on early Aβ assembly.** PICUP was applied to LMW Aβ40 analogues containing the substitutions [Asn[1]], [Asn[7]], [Asn[23]], [Asn[1,7,23]], [Gln[6]], [Gln[13]], [Gln[14]], [Gln[6,13,14]], or [Asn[1,7,13], Gln[6,13,14]]. WT Aβ40 was used as control. Molecular weight markers are shown on the *left*. The gel is representative of each of 3 independent experiments. The densitometric analysis of these experiments is available as supporting online material.

which all the Asp residues were substituted by Asn and all His residues were substituted by Gln. It should be noted that His residues are largely uncharged at pH 7.4, thus substitution of the native imidazole side-chain of His by the propylamide side-chain of the Gln residue did not significantly affect Aβ oligomerization. The gel mobilities of [Asn[1]]Aβ40 and [Asn[7]]Aβ40 oligomers were lower than those of WT Aβ40, suggesting that the oligomers formed by these analogs had a more extended structure relative to the WT oligomers. This phenomenon was seen also for [Asn[1,7,23]]Aβ40 and [Asn[1,7,23], Gln[6,13,14]]Aβ40, but was not observed for [Asn[23]]Aβ40 or for the analogues containing His substitutions. Replacement of His residues, singly or *en masse*, by Gln did not have a significant effect on the oligomer size distribution.

DISCUSSION

We have shown recently that the Aβ42 C-terminal dipeptide, Ile[41]-Ala[42], mediates formation and self-association of paranuclei (27). Ile[41] was essential for paranucleus formation, whereas Ala[42] was required for paranucleus self-association. Here, a detailed investigation of the role of amino acid side-chain structure in the C-terminal dipeptide of Aβ42 revealed how the configuration of the side-chain in position 41 controls paranucleus formation and self-assembly. An unsubstituted residue 41 Cα, even in the presence of Ala[42], oligomerized similarly to WT Aβ40. Methylation of the Cα, as in the Ala[41]-Ala[42] analogue, resulted in an oligomer distribution with features of both Aβ40 and Aβ42 oligomerization, but no high order oligomers. More typical Aβ42-like oligomerization occurred only if the Cα was alkylated with propyl or butyl groups. The *sec*-butyl side-chain of Ile[41] was particularly important for self-assembly of paranuclei into larger oligomers. The iso-propyl or iso-butyl side-chains of Val[41] and Leu[41], respectively, did not have this activity. This result suggests that it is not merely the hydrophobicity of the side-chain in position 41 that controls paranucleus association, because the iso-butyl side-chain of Leu is more hydrophobic than the *sec*-butyl side-chain of Ile (62). The requirement for the Ile residue indicates that the conformation and configuration of the side-chain in position 41 are critical for paranucleus self-association.

The C-terminal carboxylate group moderates paranucleus self-association. Thus, replacement of the charged carboxylate group by a polar, yet uncharged, carboxamide function substantially accelerated paranucleus association. Although Ala[42] is required for paranucleus association (27), the size of the side-chain in position 42 was not critically important, suggesting that it is the length of the peptide (42 *versus* 41 amino acids) rather than the nature of residue 42, which controls paranucleus self-association. The data emphasize the key role of the C-terminal dipeptide, Ile[41]-Ala[42], in determining the number and abundance of early Aβ oligomers. Essentially all of the Aβ42 analogues yielded polytonic distributions, with pentamers or hexamers being the predominant products, whereas the oligomer size distributions of Aβ40 analogues were monotonic and consistent with a rapid equilibrium among smaller oligomers (monomer through trimer or tetramer). The distinct oligomerization products produced by Aβ40 and Aβ42 may be responsible for the distinct neurotoxic activities reported recently in comparative studies of Aβ40 and Aβ42 (16). The data obtained here suggest that drugs targeting the C-terminal dipeptide of Aβ42, particularly Ile[41], could cause the longer Aβ alloform to oligomerize in the same manner as Aβ40, leading to reduced neurotoxicity and decelerated disease progression.

In addition to structural alteration in the C-terminal dipeptide, Phe[19] → Pro or Ala[21] → Gly substitutions within the Aβ CHC also affected Aβ42 oligomerization. These data show that the CHC is an important determinant controlling the size distribution of Aβ42 paranuclei, possibly through direct, intra- or intermolecular interactions with the C terminus. Substitution of Phe[19] by Pro, a modification known to abolish fibril formation (45), resulted in formation of paranuclei comprising largely hexamers. The absence of tetramers and pentamers suggests that the Pro substitution acts by stabilizing the hexamer form of the peptide. These hexamers can associate to form high molecular mass oligomers (~120–150 kDa), but the conformational rearrangements required for maturation of these high order oligomers into fibrils is inhibited by the substitution.

Relative to WT Aβ42, the Flemish variant, [Gly[21]]Aβ42, also produced a narrower paranucleus size distribution and decreased amounts of high molecular weight oligomers. Nevertheless, on average, these high molecular weight oligomers were larger than those of WT Aβ42. These results are in agreement with the reduced rate of fibrillogenesis observed for [Gly[21]]Aβ (47) and are consistent with the hypothesis that accumulation of [Gly[21]]Aβ42 paranuclei has a role in the etiology of the Flemish form of FAD. In addition, the stabilization of paranuclei increases the relative amount of soluble *versus* insoluble [Gly[21]]Aβ42. The increased solubility may facilitate the diffusion or transport of the peptide from the brain parenchyma into cerebral blood vessels, providing an explanation for the angiopathy and hemorrhagic components characteristic of the Flemish disease.

Interestingly, neither the Phe[19] → Pro nor Ala[21] → Gly sub-

stitution had a significant effect on Aβ40 oligomerization, whereas substitutions at positions 22 and 23, or truncation of N-terminal residues, had clear effects. In contradistinction, these latter structural modifications had little effect on Aβ42 oligomerization. Taken together, these data support the hypothesis that the early assembly of Aβ40 and Aβ42 occurs via distinct mechanisms (27).

The finding that substitutions of Glu^{22} or Asp^{23} facilitated formation of higher order oligomers of Aβ40 suggests that early assembly of this peptide involves, at least in part, Coulombic interactions. Recent solid-state NMR studies of Aβ fibrils provide evidence that salt bridges form between Asp^{23} and Lys^{28} and possibly between Lys^{16} and Glu^{22} (57). Our data suggest that salt bridges involving Asp^{23} and Glu^{22} may already have formed during early oligomerization of Aβ. Amino acid substitutions that affect these interactions could destabilize the structure of the resulting peptides. For example, molecular dynamics analysis of peptide solvation have shown that a $[Gln^{22}]A\beta(10–35)NH_2$ (Dutch) peptide monomer has a larger solvent-exposed hydrophobic surface area than does the WT analogue (63). Not surprisingly, a more recent comparative *in silico* analysis of peptide/water interactions of $A\beta(10–35)NH_2$ and $[Gln^{22}]A\beta(10–35)NH_2$ has shown that the Dutch peptide had weaker interactions with water than did the WT peptide (64). The side-chain of Asp^{23} was found to form hydrogen bonds, both with water and with atoms of the peptide, at an especially high frequency. This propensity is consistent with the effects of Asn substitution at this site, which we have observed causes more facile formation of higher order oligomers, both for the singly substituted Asp^{23} Aβ40 analogue and for the triply substituted Aβ40 analogue. This effect could be due to the elimination of salt bridges involving the Asp^{23} residue and because of the decrease in solvation free energy associated with substitution of the Asp^{23} acetate side-chain with an acetamide function. The propylamide substitution found in the Dutch peptide would have a similar effect on solvation free energy and thus would be expected to cause increased oligomerization, which is what we observed here experimentally. The mechanisms of action of the Arctic ($Glu^{22} \rightarrow Gly$) and Italian ($Glu^{22} \rightarrow Lys$) Aβ40 substitutions also are likely to involve destabilization of the CHC region and disruption of attractive Coulombic interactions. Our observation here that the Arctic peptide forms relatively large oligomers, and the report by Nilsberth *et al.* (25) that the Arctic substitution causes enhanced protofibril formation, are consistent with the mechanism proposed.

In addition to causing specific structural effects, amino acid substitutions can alter general properties of Aβ, especially its pI. For example, the pI of the triply substituted Aβ analogue $[Asn^{1,7,23}]A\beta40$ is 7.3 compared with ~5.2–5.5 for WT Aβ. Thus, in experiments performed at pH 7.4, this peptide was more prone to aggregation than the analogues containing individual Asp → Asn substitutions, each of which had a pI ≈ 5.8. However, the $[Asn^{1,7,23}, Gln^{6,13,14}]A\beta40$ peptide (pI ≈ 6.3) behaved similarly to $[Asn^{1,7,23}]A\beta40$, suggesting that in addition to the change in the pI, other effects contributed to the enhanced formation of higher order oligomers. For example, the conformation of $[Asn^{1,7,23}]A\beta40$ oligomers appeared to be extended relative to WT Aβ40 because their gel mobilities were lower than those of the oligomers formed by the WT peptide. This is in contrast to the gel mobilities of oligomers of analogues containing substitutions of Gly^{22}, which are larger than those of WT Aβ40. Thus, perturbation of oligomerization by amino acid substitutions may result, in part, from effects on the conformation of the specific alloform, producing a more extended or a more compact conformation. Histidine residues have been shown to be important in metal chelation by Aβ, a process that can affect the rate of fibrillogenesis (65–67). Here, substitution of His residues individually or *en masse* did not affect Aβ oligomerization, suggesting that the effects of His-mediated metal chelation come into play at later assembly stages.

In summary, our results reveal how specific regions and residues control Aβ oligomerization and show that these controlling elements differ between Aβ40 and Aβ42. The results show how each functional group in the C-terminal Ile^{41}-Ala^{42} dipeptide acts in determining the pathway through which Aβ oligomerizes. Additional evidence is provided for the existence of distinct oligomerization pathways controlling early Aβ assembly. Oligomerization of Aβ40 involves a rapid equilibrium among monomer, dimer, trimer, and tetramer, and is controlled to a significant degree by the peptide N terminus and charged residues at positions 22 and 23. In paranucleus formation by Aβ42, the predominant controlling structural elements are the C-terminal dipeptide and the CHC. Paranucleus formation depends upon the presence of a hydrophobic side-chain in amino acid 41 with a size at least as large as that of a methyl group. Paranucleus self-association is facilitated by the *sec*-butyl side-chain of Ile^{41} but not by the iso-propyl or iso-butyl side-chains of Val or Leu, respectively. The self-association step requires the presence of residue 42, and is substantially facilitated by substitution of the C-terminal carboxylate group by a carboxamide. Distinct drug design approaches for Aβ40 and Aβ42 oligomers thus may be required for efficacious treatment of specific types of FAD. The data suggest that the regions 19–21 and 41–42 are rational targets for development of assembly inhibitors for Aβ42 and that regions 1–10 and 22–23 are targets for development of Aβ40 assembly inhibitors.

Acknowledgments—We thank Drs. Erica Fradinger, Noel Lazo, Samir Maji, Dominic Walsh, and Youcef Fezoui for valuable discussions and criticism, and we thank Margaret Condron for performing peptide synthesis and purification and amino acid analysis.

REFERENCES

1. Beyreuther, K., Bush, A. I., Dyrks, T., Hilbich, C., Konig, G., Monning, U., Multhaup, G., Prior, R., Rumble, B., Schubert, W., Small, D. H., Weidemann, A., and Masters, C. L. (1991) *Ann. N. Y. Acad. Sci.* **640,** 129–139
2. Pike, C. J., Burdick, D., Walencewicz, A. J., Glabe, C. G., and Cotman, C. W. (1993) *J. Neurosci.* **13,** 1676–1687
3. Allsop, D., and Williams, C. H. (1994) *Biochem. Soc. Trans.* **22,** 171–175
4. Selkoe, D. J. (1998) *Trends Cell Biol.* **8,** 447–453
5. Kirkitadze, M. D., Bitan, G., and Teplow, D. B. (2002) *J. Neurosci. Res.* **69,** 567–577
6. Klein, W. L., Krafft, G. A., and Finch, C. E. (2001) *Trends Neurosci.* **24,** 219–224
7. Walsh, D. M., Klyubin, I., Fadeeva, J. V., Rowan, M. J., and Selkoe, D. J. (2002) *Biochem. Soc. Trans.* **30,** 552–557
8. Walsh, D. M., Tseng, B. P., Rydel, R. E., Podlisny, M. B., and Selkoe, D. J. (2000) *Biochemistry* **39,** 10831–10839
9. Walsh, D. M., Klyubin, I., Fadeeva, J. V., Cullen, W. K., Anwyl, R., Wolfe, M. S., Rowan, M. J., and Selkoe, D. J. (2002) *Nature* **416,** 535–539
10. Oda, T., Wals, P., Osterburg, H. H., Johnson, S. A., Pasinetti, G. M., Morgan, T. E., Rozovsky, I., Stine, W. B., Snyder, S. W., Holzman, T. F., Krafft, G. A., and Finch, C. E. (1995) *Exp. Neurol.* **136,** 22–31
11. Lambert, M. P., Barlow, A. K., Chromy, B. A., Edwards, C., Freed, R., Liosatos, M., Morgan, T. E., Rozovsky, I., Trommer, B., Viola, K. L., Wals, P., Zhang, C., Finch, C. E., Krafft, G. A., and Klein, W. L. (1998) *Proc. Natl. Acad. Sci. U. S. A.* **95,** 6448–6453
12. Wang, H. W., Pasternak, J. F., Kuo, H., Ristic, H., Lambert, M. P., Chromy, B., Viola, K. L., Klein, W. L., Stine, W. B., Krafft, G. A., and Trommer, B. L. (2002) *Brain Res.* **924,** 133–140
13. Gong, Y. S., Chang, L., Lambert, M. P., Viola, K. L., Krafft, G. A., Finch, C. E., and Klein, W. L. (2001) *Soc. Neurosci. Abstr.* **27,** 322.310
14. Tong, L. Q., Thornton, P. L., Balazs, R., and Cotman, C. W. (2001) *J. Biol. Chem.* **276,** 17301–17306
15. El-Agnaf, O. M., Mahil, D. S., Patel, B. P., and Austen, B. M. (2000) *Biochem. Biophys. Res. Commun.* **273,** 1003–1007
16. Dahlgren, K. N., Manelli, A. M., Stine, W. B., Jr., Baker, L. K., Krafft, G. A., and LaDu, M. J. (2002) *J. Biol. Chem.* **277,** 32046–32053
17. Walsh, D. M., Hartley, D. M., Kusumoto, Y., Fezoui, Y., Condron, M. M., Lomakin, A., Benedek, G. B., Selkoe, D. J., and Teplow, D. B. (1999) *J. Biol. Chem.* **274,** 25945–25952
18. Hartley, D. M., Walsh, D. M., Ye, C. P. P., Diehl, T., Vasquez, S., Vassilev, P. M., Teplow, D. B., and Selkoe, D. J. (1999) *J. Neurosci.* **19,** 8876–8884
19. Ward, R. V., Jennings, K. H., Jepras, R., Neville, W., Owen, D. E., Hawkins, J.,

Christie, G., Davis, J. B., George, A., Karran, E. H., and Howlett, D. R. (2000) *Biochem. J.* **348,** 137–144
20. Ye, C. P., Selkoe, D. J., and Hartley, D. M. (2003) *Neurobiol. Dis.* **13,** 177–190
21. Hsia, A. Y., Masliah, E., McConlogue, L., Yu, G. Q., Tatsuno, G., Hu, K., Kholodenko, D., Malenka, R. C., Nicoll, R. A., and Mucke, L. (1999) *Proc. Natl. Acad. Sci. U. S. A.* **96,** 3228–3233
22. Moechars, D., Dewachter, I., Lorent, K., Reverse, D., Baekelandt, V., Naidu, A., Tesseur, I., Spittaels, K., van den Haute, C., Checler, F., Godaux, E., Cordell, B., and van Leuven, F. (1999) *J. Biol. Chem.* **274,** 6483–6492
23. Mucke, L., Masliah, E., Yu, G. Q., Mallory, M., Rockenstein, E. M., Tatsuno, G., Hu, K., Kholodenko, D., Johnson-Wood, K., and McConlogue, L. (2000) *J. Neurosci.* **20,** 4050–4058
24. Pitschke, M., Prior, R., Haupt, M., and Riesner, D. (1998) *Nat. Med.* **4,** 832–834
25. Nilsberth, C., Westlind-Danielsson, A., Eckman, C. B., Condron, M. M., Axelman, K., Forsell, C., Stenh, C., Luthman, J., Teplow, D. B., Younkin, S. G., Naslund, J., and Lannfelt, L. (2001) *Nat. Neurosci.* **4,** 887–893
26. Bitan, G., Lomakin, A., and Teplow, D. B. (2001) *J. Biol. Chem.* **276,** 35176–35184
27. Bitan, G., Kirkitadze, M. D., Lomakin, A., Vollers, S. S., Benedek, G. B., and Teplow, D. B. (2003) *Proc. Natl. Acad. Sci. U. S. A.* **100,** 330–335
28. Fancy, D. A., and Kodadek, T. (1999) *Proc. Natl. Acad. Sci. U. S. A.* **96,** 6020–6024
29. Fancy, D. A., Denison, C., Kim, K., Xie, Y. Q., Holdeman, T., Amini, F., and Kodadek, T. (2000) *Chem. Biol.* **7,** 697–708
30. Walsh, D. M., Lomakin, A., Benedek, G. B., Condron, M. M., and Teplow, D. B. (1997) *J. Biol. Chem.* **272,** 22364–22372
31. Garzon-Rodriguez, W., Sepulveda-Becerra, M., Milton, S., and Glabe, C. G. (1997) *J. Biol. Chem.* **272,** 21037–21044
32. Lomakin, A., Chung, D. S., Benedek, G. B., Kirschner, D. A., and Teplow, D. B. (1996) *Proc. Natl. Acad. Sci. U. S. A.* **93,** 1125–1129
33. van Nostrand, W. E., Melchor, J. P., Cho, H. S., Greenberg, S. M., and Rebeck, G. W. (2001) *J. Biol. Chem.* **276,** 32860–32866
34. Fezoui, Y., Hartley, D. M., Harper, J. D., Khurana, R., Walsh, D. M., Condron, M. M., Selkoe, D. J., Lansbury, P. T., Fink, A. L., and Teplow, D. B. (2000) *Amyloid: Int. J. Exp. Clin. Invest.* **7,** 166–178
35. Kotzyba-Hibert, F., Kapfer, I., and Goeldner, M. (1995) *Angew. Chem. Int. Ed. Engl.* **34,** 1296–1312
36. Hendriks, L., van Duijn, C. M., Cras, P., Cruts, M., van Hul, W., van Harskamp, F., Warren, A., McInnis, M. G., Antonarakis, S. E., Martin, J. J., Hofman, A., and van Broeckhoven, C. (1992) *Nat. Genet.* **1,** 218–221
37. Levy, E., Carman, M. D., Fernandez-Madrid, I. J., Power, M. D., Lieberburg, I., van Duinen, S. G., Bots, G. T. A. M., Luyendijk, W., and Frangione, B. (1990) *Science* **248,** 1124–1126
38. Tagliavini, F., Rossi, G., Padovani, A., Magoni, M., Andora, G., Sgarzi, M., Bizzi, A., Savioardo, M., Carella, F., Morbin, M., Giaccone, G., and Bugiani, O. (1999) *Alzheimer's Rep.* **2,** (suppl.), S28
39. Kamino, K., Orr, H. T., Payami, H., Wijsman, E. M., Alonso, E., Pulst, S. M., Anderson, L., O'dahl, S., Nemens, E., White, J. A., Sadovnick, A. D., Ball, M. J., Kayue, J., Warren, A., McInnis, M., Antonarakis, S. T., Korenberg, J. R., Sharma, V., Kukull, W., Larson, E., Heston, L. L., Martin, G. M., Bird, T. D., and Schellenberg, G. D. (1992) *Am. J. Hum. Genet.* **51,** 998–1014
40. Grabowski, T. J., Cho, H. S., Vonsattel, J. P. G., Rebeck, G. W., and Greenberg, S. M. (2001) *Ann. Neurol.* **49,** 697–705
41. Teplow, D. B. (1998) *Amyloid: Int. J. Exp. Clin. Invest.* **5,** 121–142
42. Selkoe, D. J. (2001) *Physiol. Rev.* **81,** 741–766
43. Clements, A., Allsop, D., Walsh, D. M., and Williams, C. H. (1996) *J. Neurochem.* **66,** 740–747
44. Miravalle, L., Tokuda, T., Chiarle, R., Giaccone, G., Bugiani, O., Tagliavini, F., Frangione, B., and Ghiso, J. (2000) *J. Biol. Chem.* **275,** 27110–27116
45. Wood, S. J., Wetzel, R., Martin, J. D., and Hurle, M. R. (1995) *Biochemistry* **34,** 724–730
46. Teplow, D. B., Lomakin, A., Benedek, G. B., Kirschner, D. A., and Walsh, D. M. (1997) in *Alzheimer's Disease: Biology, Diagnosis and Therapeutics* (Iqbal, K., Winblad, B., Nishimura, T., Takeda, M., and Wisniewski, H. M., eds) pp. 311–319, John Wiley & Sons Ltd., Chichester, UK
47. Walsh, D. M., Hartley, D. M., Condron, M. M., Selkoe, D. J., and Teplow, D. B. (2001) *Biochem. J.* **355,** 869–877
48. Teller, J. K., Russo, C., Debusk, L. M., Angelini, G., Zaccheo, D., Dagnabricarelli, F., Scartezzini, P., Bertolini, S., Mann, D. M. A., Tabaton, M., and Gambetti, P. (1996) *Nat. Med.* **2,** 93–95
49. Saido, T. C., Iwatsubo, T., Mann, D., Shimada, H., Ihara, Y., and Kawashima, S. (1995) *Neuron* **14,** 457–466
50. Haass, C., Hung, A. Y., Selkoe, D. J., and Teplow, D. B. (1994) *J. Biol. Chem.* **269,** 17741–17748
51. Haass, C., Schlossmacher, M. G., Hung, A. Y., Vigo-Pelfrey, C., Mellon, A., Ostaszewski, B. L., Lieberburg, I., Koo, E. H., Schenk, D., Teplow, D. B., and Selkoe, D. J. (1992) *Nature* **359,** 322–325
52. Pike, C. J., Overman, M. J., and Cotman, C. W. (1995) *J. Biol. Chem.* **270,** 23895–23898
53. Larner, A. J. (1999) *Neurobiol. Aging* **20,** 65–69
54. Teplow, D. B. (1999) *Neurobiol. Aging* **20,** 71–73
55. Saido, T. C., Yamao-Harigaya, W., Iwatsubo, T., and Kawashima, S. (1996) *Neurosci. Lett.* **215,** 173–176
56. Russo, C., Saido, T. C., DeBusk, L. M., Tabaton, M., Gambetti, P., and Teller, J. K. (1997) *FEBS Lett.* **409,** 411–416
57. Petkova, A. T., Yoshitaka, I., Balbach, J. J., Antzutkin, O. N., Leapman, R. D., Delaglio, F., and Tycko, R. (2002) *Proc. Natl. Acad. Sci. U. S. A.* **99,** 16742–16747
58. Wood, S. J., Maleeff, B., Hart, T., and Wetzel, R. (1996) *J. Mol. Biol.* **256,** 870–877
59. Barrow, C. J., Yasuda, A., Kenny, P. T. M., and Zagorski, M. (1992) *J. Mol. Biol.* **225,** 1075–1093
60. Tomski, S. J., and Murphy, R. M. (1992) *Arch. Biochem. Biophys.* **294,** 630–638
61. Kirkitadze, M. D., Condron, M. M., and Teplow, D. B. (2001) *J. Mol. Biol.* **312,** 1103–1119
62. Vandewaterbeemd, H., Karajiannis, H., and Eltayar, N. (1994) *Amino Acids* **7,** 129–145
63. Massi, F., Peng, J. W., Lee, J. P., and Straub, J. E. (2001) *Biophys. J.* **80,** 31–44
64. Massi, F., and Straub, J. E. (2003) *J. Comput. Chem.* **24,** 143–153
65. Yang, D. S., McLaurin, J., Qin, K. F., Westaway, D., and Fraser, P. E. (2000) *Eur. J. Biochem.* **267,** 6692–6698
66. Liu, S. T., Howlett, G., and Barrow, C. J. (1999) *Biochemistry* **38,** 9373–9378
67. Atwood, C. S., Moir, R. D., Huang, X. D., Scarpa, R. C., Bacarra, N. M. E., Romano, D. M., Hartshorn, M. K., Tanzi, R. E., and Bush, A. I. (1998) *J. Biol. Chem.* **273,** 12817–12826

Protein Structure and Folding:

Elucidation of Primary Structure Elements Controlling Early Amyloid β-Protein Oligomerization

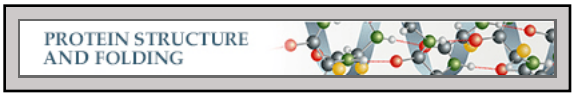

Gal Bitan, Sabrina S. Vollers and David B. Teplow

J. Biol. Chem. 2003, 278:34882-34889.
doi: 10.1074/jbc.M300825200 originally published online July 2, 2003
